



## Experimental Investigation of RC Exterior Beam Column Connection with Eccentric Beam Subjected to Reversible Quasi Static Loads

Ahmed G. Asran<sup>a</sup>, Hassan H. EL-Esnawi<sup>b</sup>, Sabry Fayed<sup>c\*</sup>

<sup>a</sup> Prof. of Concrete Structures, Faculty of Engineering, Azhar University, Egypt.

<sup>b</sup> Associate Professor, Civil Engineering Department, Faculty of Engineering, Azhar University, Egypt.

<sup>c</sup> Assistant lecturer, Civil Engineering Department, Kafrelshiekh University, Egypt.

Received 18 February 2017; Accepted 20 April 2017

### Abstract

Insufficiency of the Beam Column Joint (BCJ) caused structures failures particularly in case of the earthquakes. In most of the buildings, the beam center line was not aligned with the column center line. So, the effect of the eccentricity of the beam was studied in this article. Behaviour of reinforced concrete (RC) eccentric beam-column joint under reversible cyclic loading was investigated experimentally. The experimental program is one specimen. The specimen consisted of column and beam. The column divided into symmetry two parts (upper and lower parts). The beam fixed in middle of the column and it was free end. The main parameter was the effect of the eccentricity of the beam center line about the column center on behaviour of RC BCJ. The specimen was tested under reversible ten cycles. The horizontal displacement for the column and the vertical deflection at free end of the beam were recorded at each cycle. The crack pattern of the tested specimen was studied at every cycle in details. It was noticed that the eccentricity of the beam has concentrated more stresses on the joint side close to the eccentricity. The failure took place at the joint due to its weakness.

*Keywords:* Experimental Work; Reinforced Concrete Beam Column Joints; Cyclic Loading; Crack Propagation.

### 1. Introduction

Behavior of RC BCJ is very important because most of the structures subjected to earthquakes failed in the connections between the columns and the beams. The eccentric RC BCJ has a dangerous effect more than the concentric the RC BCJ. This was because that the eccentricity transmitted more stresses on one side without the other side. So the American code (ACI 352R-2 [1]) recommended by studying of the eccentric connections subjected to cyclic loading. A case study on pre 1970s constructed concrete exterior beam-column joints was studied by Ravi Kiran and Giovacchino Genesio [2]. Angelo Masi and et al. [3] induced an experimental tests and numerical simulations that were carried out on an external RC beam-column joint under seismic loads. Cyclic tests carried out on full-scale joint specimens. The main parameter was effect the axial compression column load. It was noticed that the value of the axial load acting on the column can change the collapse mode.

The effect of eccentricity on the seismic behavior of exterior beam-to-column connections was studied by Burcu Burak and James k. Wight [4]. Three (3/4-scale) exterior reinforced concrete beam-column-slab connections were tested under reversed cyclic loading. Cyclic loading tests of six full-scale RC beam-column connections were investigated by Rajesh Prasad Dhakal and et al. [5]. Many researchers introduced a lot of papers that studied behavior

\* Corresponding author: [sabrielmorsi@yahoo.com](mailto:sabrielmorsi@yahoo.com)

➤ This is an open access article under the CC-BY license (<https://creativecommons.org/licenses/by/4.0/>).

of RC BCJ under cyclic loads such as A.M. Elsouiri and et al. [6], Constantin and et al. [7], and Jianping FU and et al. [8].

Prakash panjwani and S.k. Dubey [10] induced a review article of the proposed theories associated with the behaviour of RC BCJ because that understanding the joint behaviour is essential in training proper findings in the design of connection. The researcher discussed about the seismic actions on various types of connections and highlights the critical parameters that affect connection performance with special reference to bond and shear transfer. Er. Khairnar Nilesh K and et al. [11] presented an experimental investigation of interior RC BCJ under torsional loading. In the current study, the behavior of RC BCJ with eccentric beam was induced. The effect of the eccentricity of the beam on the failure modes was investigated in details. The deformation behavior of the connection was studied. The experimental program was illustrated in section 2. Specimens detailed in section 2-1 while section 2-2 and section 2-3 described material properties of used materials and Test set-up used in this experiment. The loading cyclic technique was induced in section 2-4. Experimental Results and Discussion proposed in section 3 while conclusion written in section 4. Finally, section 5 illustrated the sources used in this study.

## 2. Experimental Program

### 2.1. Specimen Description

The experimental program consisted of one reduced scale reinforced concrete (RC) beam column joint (BCJ) (1/3 scale model). In the current study, an exterior isolated beam-column joint as shown in Figure 1. was considered. It consisted of half the height of a column on each side of the joint and part of the beam up to 50% of the span, which corresponded to the points of contra-flexure in beam and column under lateral loads. Symmetric boundary conditions were maintained at both ends of the column for isolation of a single unit of beam-column connections. A typical full-scale residential building with floor to floor height ( $h_c$ ) as 3.9 m and the beam ( $L_b$ ) of 3.6 m effective span was considered. The connection was scaled down to 1/3 size for the experimental work as shown in Figure 2. The Egyptian code [9] was used in design of the specimen. The column has a cross section of  $100 \times 200$  mm (see in Figure 2.). The total height of the column was 1300 mm. The beam had 100 mm width and 200 mm depth. The column was reinforced by 4D12 mm in longitudinal direction and 12D6 mm/m in the transversal direction except the joint panel. The shear reinforcement of joint panel was 1D6 mm. For the beam, the top and bottom main longitudinal bars were 2D12 in longitudinal direction while 10D6/m were used as vertical stirrups. The stirrups were started from the column face. The embedded length of lower and upper main steel of the beam was 245 mm from the critical section of the flexure. The typical concrete dimensions for all parts of the specimen are shown in Figure 2. The reinforcement details for tested specimen are illustrated in Figure 3. The casting steps of concrete inside wood form showed in Figure 4.

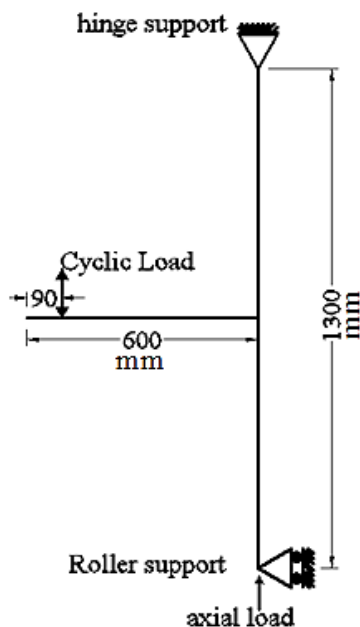


Figure 1. Exterior isolated beam-column joint

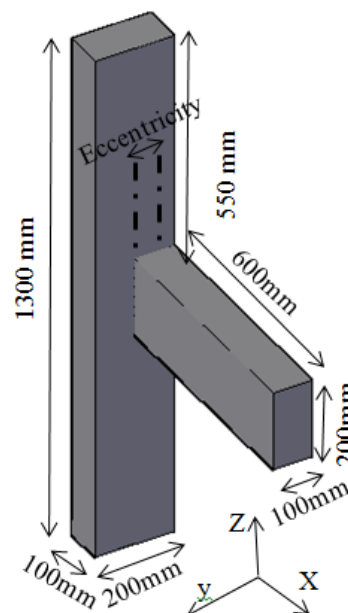


Figure 2. Typical dimension of the tested specimen

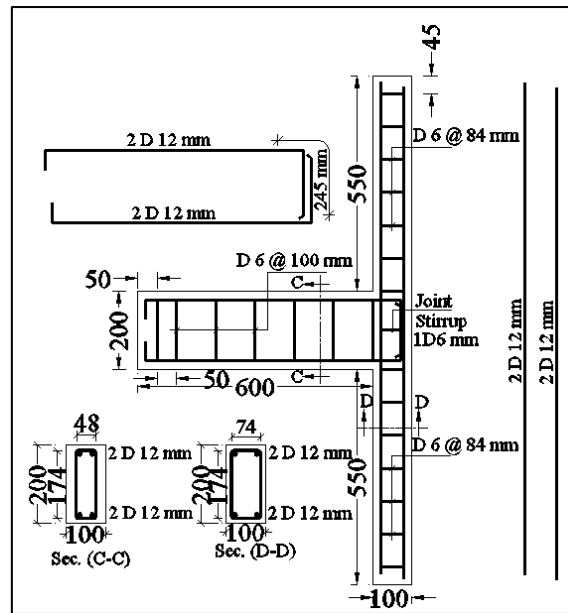


Figure 3. Reinforcement details of the tested specimen



Step 1: Reinforcement shape



Step 2: Casting of the column



Step 3: Fixation and Casting of the beam

Figure 4. Steps of the specimen casting

## 2.2. Material Properties

The normal strength concrete mixture was used in casting of the specimen. The mix proportions for 1 m<sup>3</sup> were listed in Table 1. The crushed dolomite had maximum aggregate size of 15 mm, and the water-cement ratio (w/c) was 0.50. The super plasticizer was added to the mix in order to increase workability and strength of concrete and its ratio was 1% of cement weight. To determine the compressive strength of the used concrete, the standard cubic (150 × 150 × 150 mm) were used according to the Egyptian code [9]. Average 28-day concrete cubic strength was 35 MPa. Tension test were carried out on the reinforcing bars. The yield strength was 410 MPa and 250 MPa for bar diameters of 12mm and 6mm respectively.

Table 1. Concrete Mix Proportions per m<sup>3</sup>

Portland cement (Kg)	Sand (Kg)	Crushed dolomite (Kg)	Water/Cement	Admixture (liters)
350	637	1295	0.5	3.5

### 2.3. Test Set-up and Instrumentation

The test set-up showed in Figure 5. was used for experimental investigation. The upper support of the column was hinged support in order to allow rotation about y-axes only. Bolt (1) showed in Figure 5. added to upper support in order to prevent the horizontal movement of the column in plan and out of plane. While the lower support was roller to prevent the horizontal movement and allowed the vertical movement. Bolt (2) showed in Figure 5. used to prevented the horizontal movement in all directions. A dial gauge with maximum displacement 50 mm was used to measure the vertical deflection at free end of the beam ( $\Delta_1$ ). The horizontal movement of the column was recorded by other displacement gauge ( $\Delta_2$ ) at mid-point of upper column. Its accuracy was 0.01 mm. Figure 6. shows the horizontal displacement ( $\Delta_2$ ) of the column and the vertical deflection ( $\Delta_1$ ) of the beam.

A three hydraulic jacks were used in this setup. Their capacity was 250 KN. The first hydraulic jack was used to apply 100 KN as a constant axial compression load on lower end of the column during the test to represent the gravity load. The compression load was applied before the test and it was kept constant during the test. The second and the third jacks were used to apply cyclic load at the free end of the beam. During the test, the vertical beam tip deflection and crack propagation were recorded at each cycle.

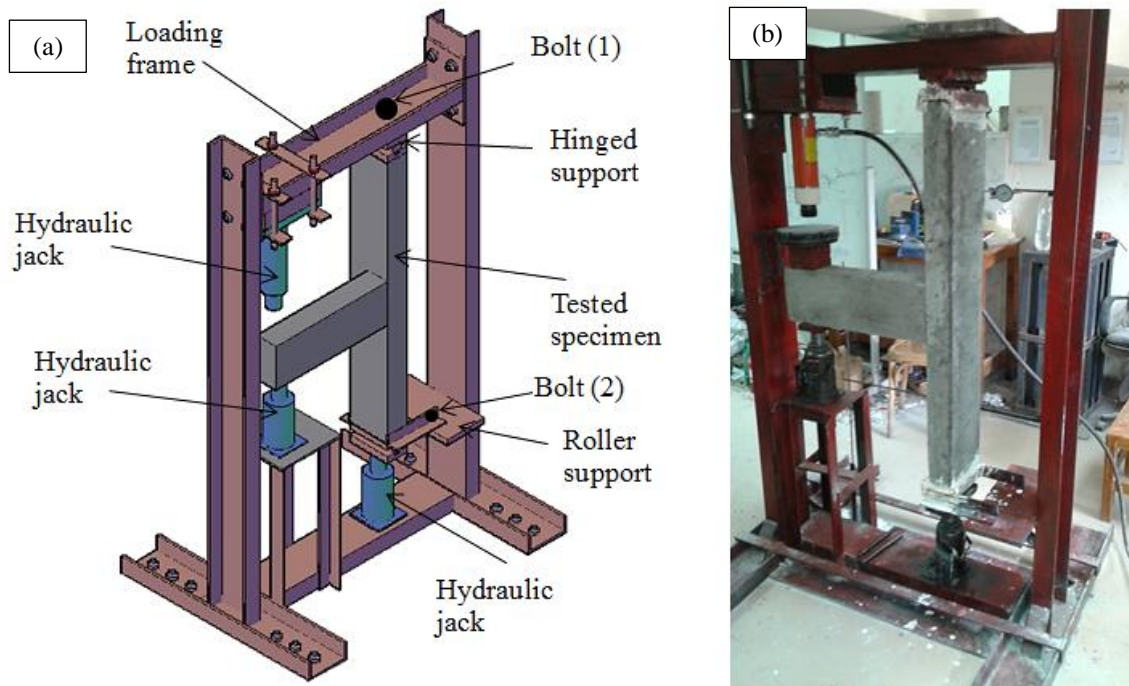


Figure 5. (a) Schematic diagram of the test set-up (b) Actual testing arrangement of the specimen

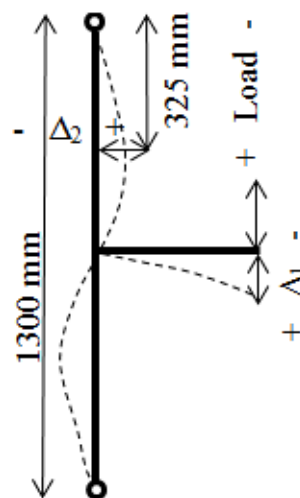


Figure 6. Measurements of the specimen

### 2.4. Cyclic Loading Sequence

The two hydraulic jacks placed at the beam were used to apply the reversible cyclic loading (see in Figure 5.). In the current article, the loading cyclic history is presented in Figure 7. The total numbers of cycles was ten cycle. Each

cycle was larger than the previous one by 2 mm. The first cycle was divided into two stages. For the first stage, the free end of the beam loaded down ward by the upper jack until the vertical displacement reached to 2 mm. the load of the upper jack was released. The lower jack was used to retain the beam to the initial position. For the second stage, the free end of the beam loaded up ward using the lower jack until the vertical displacement reached to -2 mm. the load of the lower jack was removed. The upper jack was used to retain the beam to the horizontal initial position. Same procedure was carried out in the followed cycles. For example, the 6<sup>th</sup> cycle started at 0 mm to +12 mm to 0 mm to -12 mm to 0 mm.

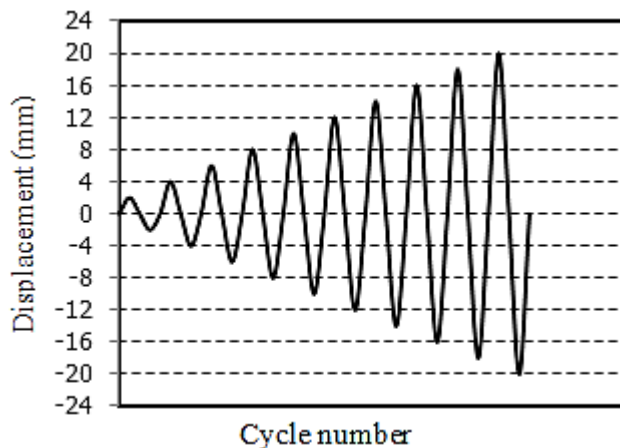


Figure 7. Cyclic loading histories

### 3. Experimental Results and Discussion

#### 3.1. Crack Pattern and Failure Modes

The crack propagation at each cycle end due to cyclic loading is presented in Figures 8 to 19. In the early stage of cyclic loading, the first cracks in the specimen mainly developed at the beam-column joint interface as shown in Figure 8. The 1<sup>st</sup> cycle ended at the load of 9 KN down word. In this cycle, the cracks number was two cracks. The first took place at the beam-column joint interface while the second occurred at the top side of the beam due to flexural stresses. The BCJ was divided into four zones A, B, C, and D as shown in the following figures.

With increasing of the cyclic loading rate, the cracks spread towards the weakest zone. For the second cycle, the load reached to 13 KN down ward then it was released. Same load of 13 KN affected on the beam up ward and it was removed. The previous two flexural cracks extended in this cycle. The first crack extended to the joint from the front (zone A) and it extended to the joint from the side (zone B) as shown in Figure 9 and 10. showed cracks shape when the loading direction was inverted up word. Same cracks were appeared on the opposite sides in addition to one crack in the joint from the side (zone C). It was shown that the cracks appeared on both sides of the joint (zones B and C). But the cracks on zone B were bigger than the cracks on zone C. The eccentricity of the beam toward zone B was the reason. This eccentricity transmitted more stresses on the side than other side.

Both Figure 11 and 12. showed the added cracks of the tested specimen at the 3<sup>rd</sup> cycle ending either the load was loaded down word or up word. The flexural cracks of the beam were increased either in the depth or the number. This was because the load value increased to 14 KN at the end of this cycle. The cracks concentrated on the side of the joint (zone B) in addition to the cracks increased in the face of the joint (zone A). When the load directed up word at 14 KN, the first crack appeared at the joint from the back (zone D) as shown in Figure 12b.

Figure 13. showed the cracks propagation of the tested specimen at the 4<sup>th</sup> cycle ending. It was notice that the length and numbers of the cracks in the joint (zone A, B, C, and D) increased particularly in the zone B. also the flexural cracks depth of the beam was increased because the load value increased to 14.5 KN in this cycle.

Figure 14. showed the crack pattern of the tested specimen after the 5<sup>th</sup> cycle ending. The load reached to 16 KN at the end of the cycle. The cracks were increased in all sides of the joint. The crack propagation was the biggest in zone B and it was the least in zone C due to the beam eccentricity toward zone B. It showed that all cracks of the joint were started from one point of the six points which marked in Figure 14. This may be because that the load transmitted from the beam to the column through these six points.

Figure 15. showed the crack pattern of the tested specimen after the 6<sup>th</sup> cycle ending. The load still at 16.4 KN with the end of the cycle. The cracks took placed at the upper part of the column as shown in Figure 15b. For the back of the joint (zone D), the horizontal cracks extended to full width of the column. The value of the load was 17.4 KN at the 7<sup>th</sup> cycle as shown in Figure 16. The maximum load was occurred at this cycle. One crack started from point 3 (see Figure 14.) toward up ward on the column. When the displacement increased to 16 mm in the 8<sup>th</sup> cycle, the load capacity decreased to 16.8 KN as shown in Figure 17. Same crack extended from point 3 increased vertically upward.

The cracks in the side and the back of the joint were developed in its numbers. In the 9<sup>th</sup> cycle (see in Figure 18.), the cracks propagated speedily in all parts of the joint. Also the cracks spread above and down the beam. The load capacity decreased to 15 KN in this cycle. Figure 19. showed the cracks pattern of the last cycle. More views were recorded for all parts of the tested specimen. The maximum load in this cycle was 14 KN. The concrete crashed in the part of the column that placed above the beam directly. The widest cracks were taken placed at the side of the joint (zone B). The failure took placed in zone B which expected position.



Figure 8. Crack pattern of specimen after the 1<sup>st</sup> cycle ending when the load toward down ward

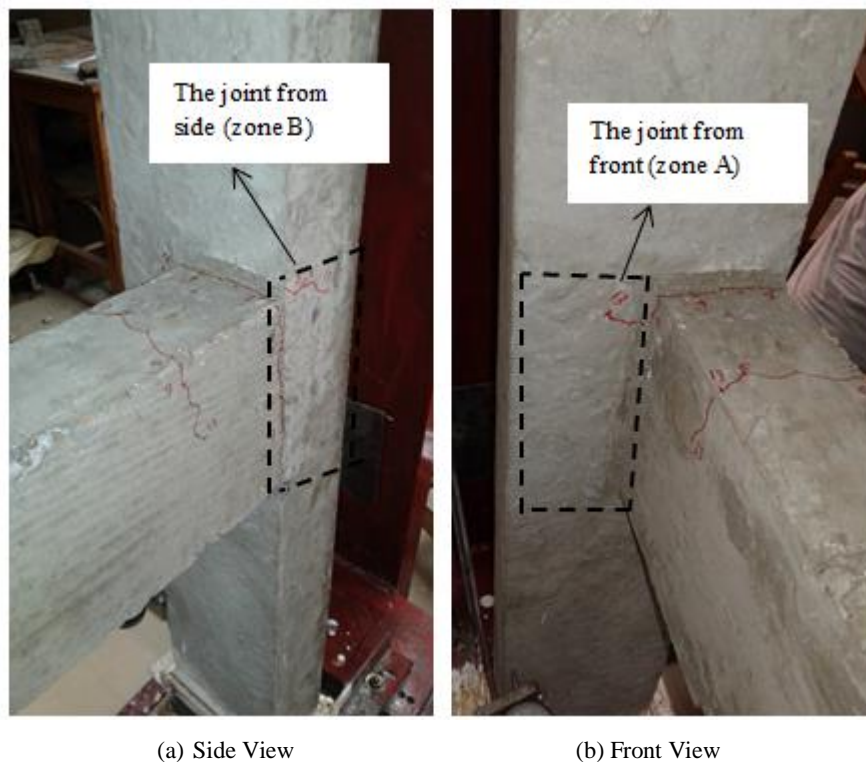


Figure 9. Crack pattern of specimen after the 2<sup>nd</sup> cycle ending when the load toward down ward



Figure 10. Crack pattern of specimen after the 2<sup>nd</sup> cycle ending when the load toward upward



Figure 11. Crack pattern of specimen after the 3<sup>rd</sup> cycle ending when the load toward down ward

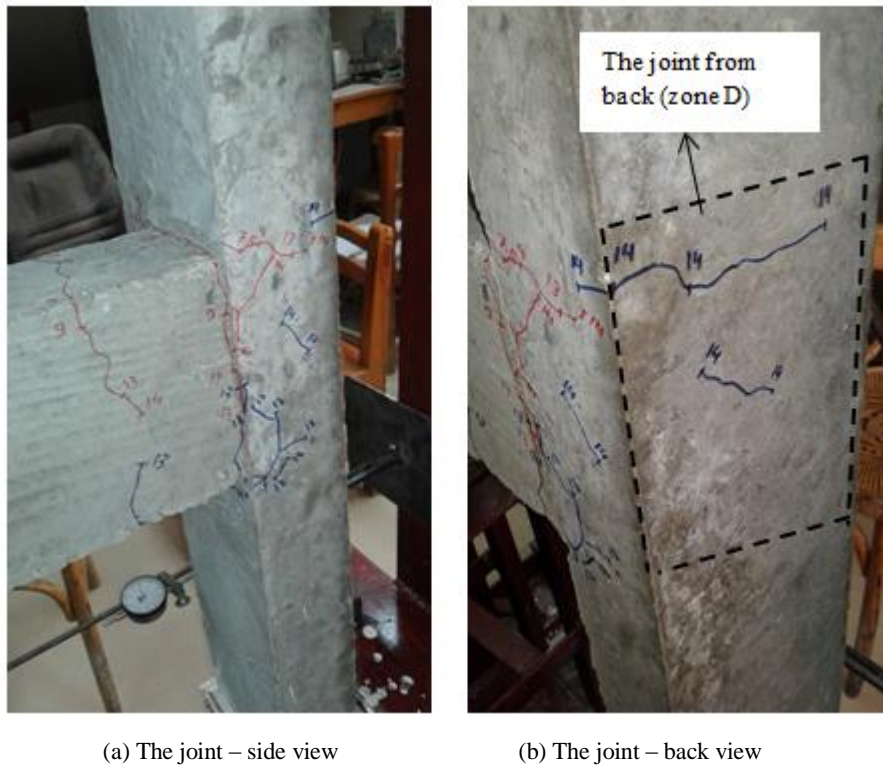


Figure 12. Crack pattern of specimen after the 3<sup>rd</sup> cycle ending when the load toward upward

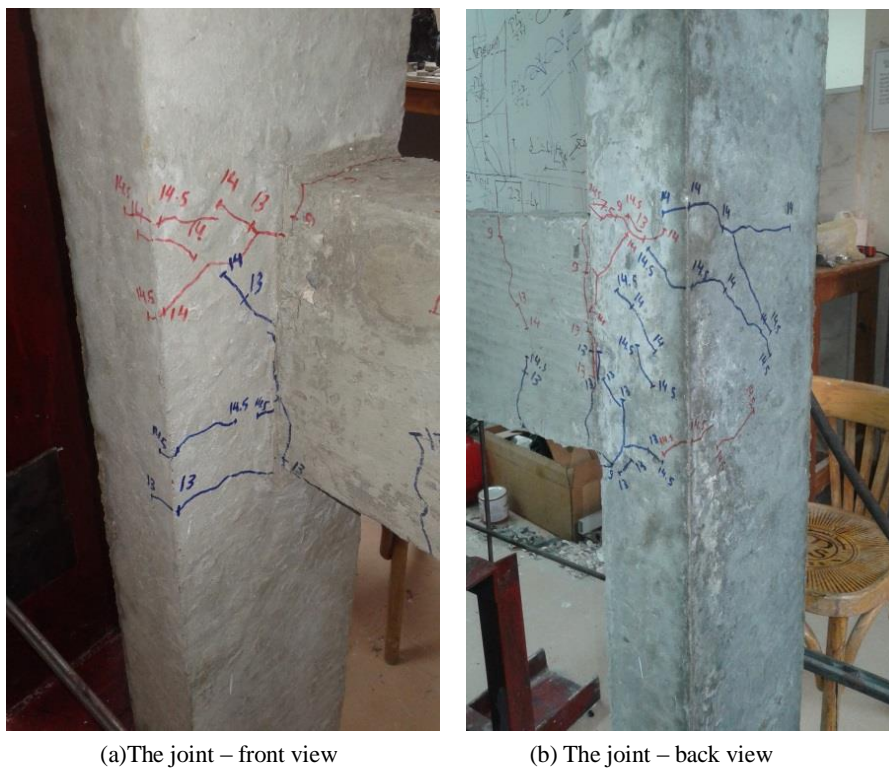
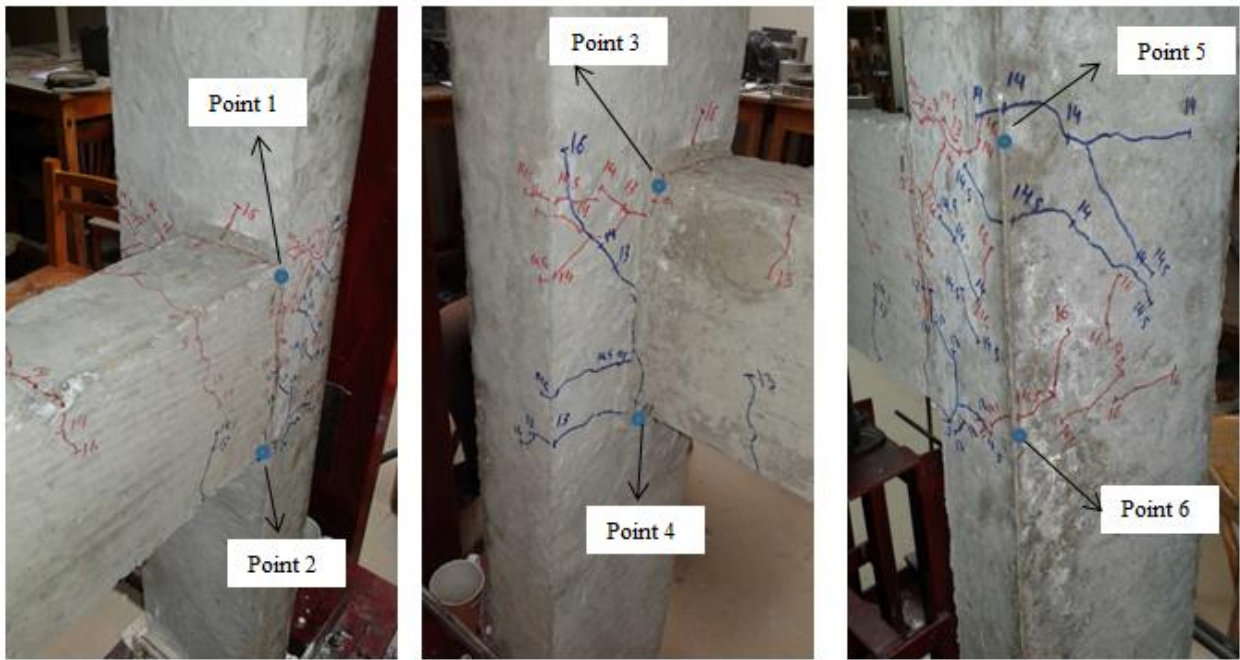


Figure 13. Crack pattern of specimen after the 4<sup>th</sup> cycle ending





(a) The joint – side view

(b) The joint – front view

(c) The joint – back view

Figure 14. Crack pattern of specimen after the 5<sup>th</sup> cycle ending (up and down loading)



(a) The joint – front view

(b) The joint – back view

(c) The column – side view

Figure 15. Crack pattern of specimen after the 6<sup>th</sup> cycle ending



(a) The joint – front view

(b) The joint – back view

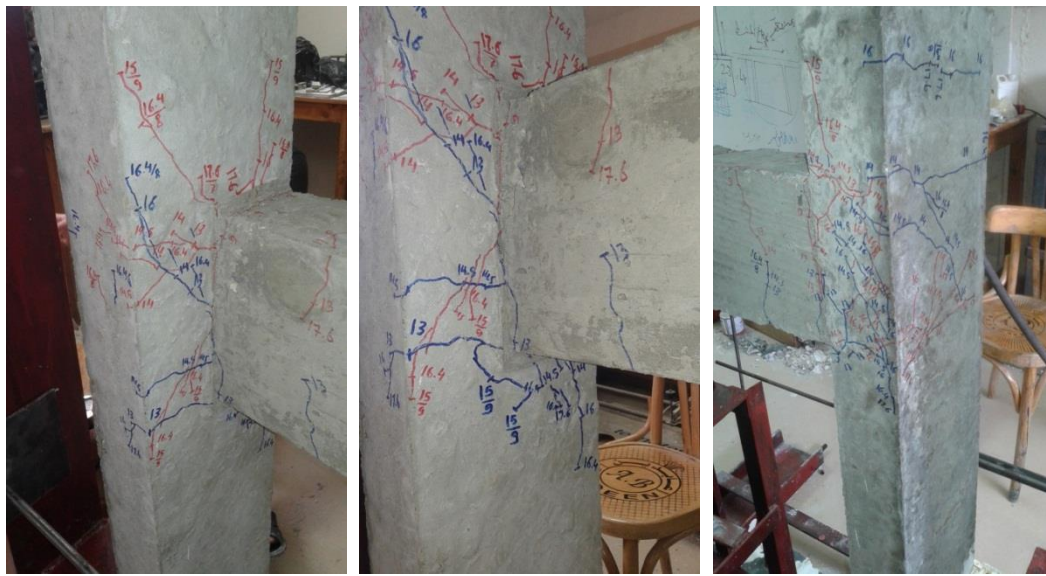
**Figure 16. Crack pattern of specimen after the 7<sup>th</sup> cycle ending**



(a) The joint – front view

(b) The joint – back view

**Figure 17. Crack pattern of specimen after the 8<sup>th</sup> cycle ending**



(a) The joint – front view

(b) The joint – bottom view

(c) The joint – back view

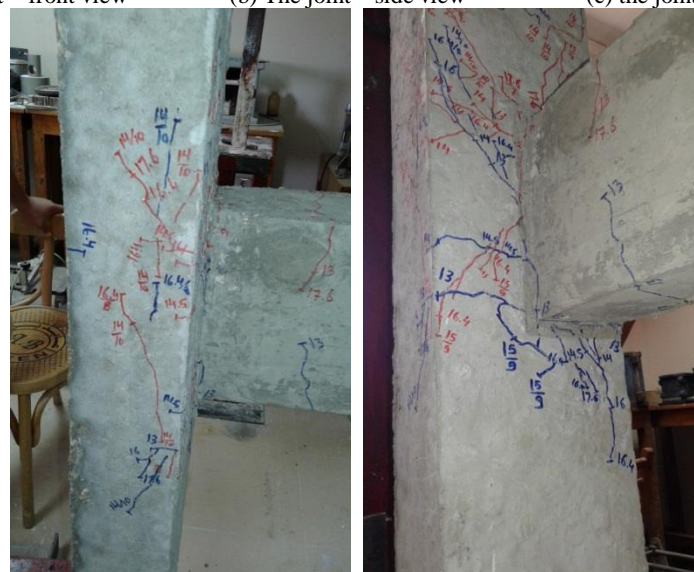
Figure 18. Crack pattern of specimen after the 9<sup>th</sup> cycle ending



(a) The joint – front view

(b) The joint – side view

(c) The joint – back view



(d) The joint – side view

(e) The joint – bottom view

Figure 19. Crack pattern of the specimen after the 10<sup>th</sup> cycle ending

### 3.2. Deformation Behavior of The Tested Specimen

The relationship between the load and the vertical deflection ( $\Delta_1$ ) of the beam end for all cycles was shown in Figure 20. This figure included more curves, so the curves were drawn in five figures. The load-deflection relationship consisted of positive 10 cycle plus negative 10 cycle. In order to make a comparison between two cycles, each two cycle was drawn in a single figure. Figures 21-25. are showed the curves for all cycles in details. For the first cycle, the curve begins at 0 mm deflection then increased gradually until reached to the maximum displacement (2 mm). The load was removed slowly and it was retained back to 0 KN again. It was noticed that the deflection was not retained back to 0 mm but it kept part of the displacement at cycle positive end. The values of remained displacement at each cycle end at 0 KN were illustrated in the Figures 21-25. Often, the remained displacement in any cycle was higher than the remained displacement in the previous cycle. This might be due to cracks spread in the consecutive cycles. The slope of the curve in any current cycle was less than the curve slope in the previous cycle. On the other hand, as cycle number increased, the rate of deflection increased at the same level of loading. This may be due to decreasing of the rigidity with more cycles. Other reason was that the cracks propagation in any cycle more than the previous. For all cycles, it was showed that the deflection value at a given load during increasing of loading was less than the deflection value at the same load during removing of loading. Figure 26. showed the relationship between cycle end displacement and the corresponding load for same cycle. It was found that the capacity of the tested specimen increased gradually from the 1<sup>st</sup> cycle to the 7<sup>th</sup> cycle until it reached to the peak then it was decreased.

The horizontal movement ( $\Delta_2$ ) of upper part of the column at height middle was recorded (see in Figure 6.). The positive value of the load was toward down ward direction. The positive value of  $\Delta_2$  means that the movement to the right (see in Figure 6.). Figure 27. showed the relationship between the load and horizontal displacement  $\Delta_2$  for the 1<sup>st</sup> cycle and the 2<sup>nd</sup> cycle. As the load increased, the  $\Delta_2$  value increased until ending of maximum displacement of cycle. When the load was removed slowly, the  $\Delta_2$  decreased. During removing of the load, the displacement retained speedily more than before the loading. At the 1<sup>st</sup> cycle end, the maximum movement of the column ( $\Delta_2$ ) reached to  $10 \times 0.01$  mm. each cycle divided into two parts of the loading; the first is displacement from 0 mm to 2 mm then removing of the load. The second is displacement from 0 to -2 mm then removing of the load. For the 2<sup>nd</sup> cycle, the maximum value of  $\Delta_2$  was  $24 \times 0.01$  mm at the cycle end. The slope of the curve of the 1<sup>st</sup> cycle was equal with the curve slope of the 2<sup>nd</sup> cycle approximately. The curves of the 3<sup>rd</sup> and the 4<sup>th</sup> cycle are drawn in Figure 28. Both of two curves have same trend and its values. For both two cycles, the maximum of  $\Delta_2$  is  $40 \times 0.01$  mm. The remained displacement at end of the first half of cycle was  $-32 \times 0.01$  mm for the 3<sup>rd</sup> cycle while it was  $-48 \times 0.01$  mm for the 4<sup>th</sup> cycle. Figure 29. showed the load versus  $\Delta_2$  for the 5<sup>th</sup> and the 6<sup>th</sup> cycles. The increasing rate of deflection of the 6<sup>th</sup> cycle was higher than deflection rate of the 5<sup>th</sup> cycle. The maximum displacement of  $\Delta_2$  of the 6<sup>th</sup> cycle was  $56 \times 0.01$  mm while it was  $40 \times 0.01$  mm for the 5<sup>th</sup> cycle. For the 7<sup>th</sup> cycle and the 8<sup>th</sup> cycle, the curves of deformation were showed in Figure 30. The maximum value of  $\Delta_2$  for the 8<sup>th</sup> cycle was higher than the  $\Delta_2$  of the 7<sup>th</sup> cycle. It was found that the linear behavior of the curve during removing of the load was showed for all cycles. Figure 31. showed load-deflection curve of the 9<sup>th</sup> and the 10<sup>th</sup> cycle. The maximum of  $\Delta_2$  for both the 9<sup>th</sup> and the 10<sup>th</sup> cycle was  $56 \times 0.01$  mm. The peaks of all cycles were drawn in Figure 32. It was showed that the peak of both the 5<sup>th</sup> cycle and the 6<sup>th</sup> cycle were the worst in all cycles. The maximum value of  $\Delta_2$  was  $64 \times 0.01$  mm during the experiment. To make a comparison between all cycles, the curves of all cycles were drawn in Figure 33. The slope of curve for any cycle was less than the curve slope for the previous cycle. For all cycles, all curves were straight lines during load removing.

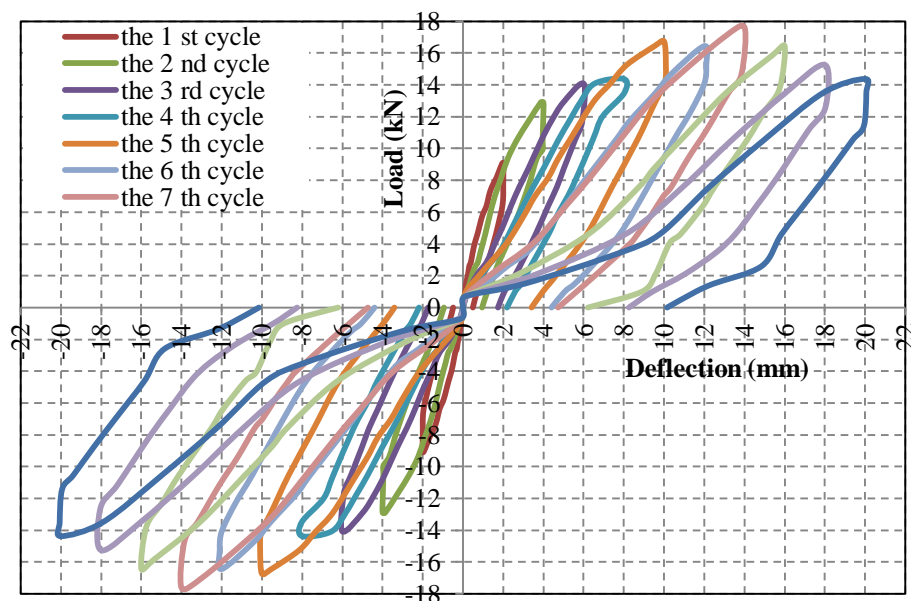


Figure 20. Load- deflection relationships of all cycles for the tested specimen- $\Delta_1$

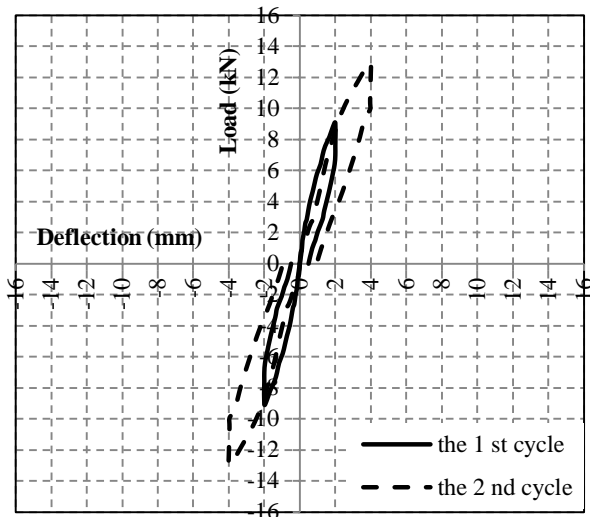


Figure 21. Load- deflection curve of the 1<sup>st</sup> and 2<sup>nd</sup> cycles -  $\Delta_1$

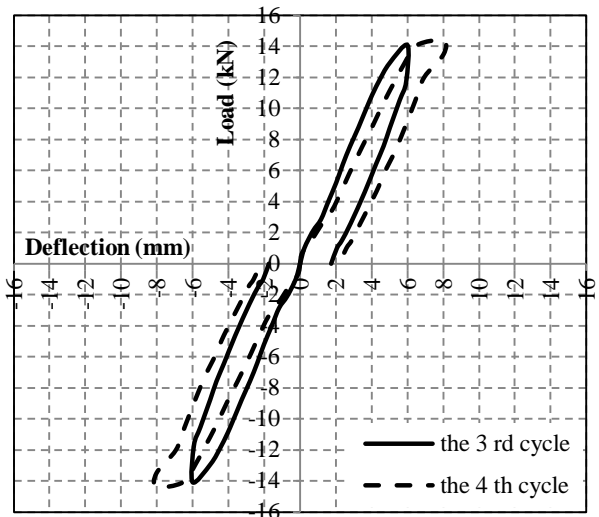


Figure 22. Load- deflection curve of the 3<sup>rd</sup> and 4<sup>th</sup> cycles -  $\Delta_1$

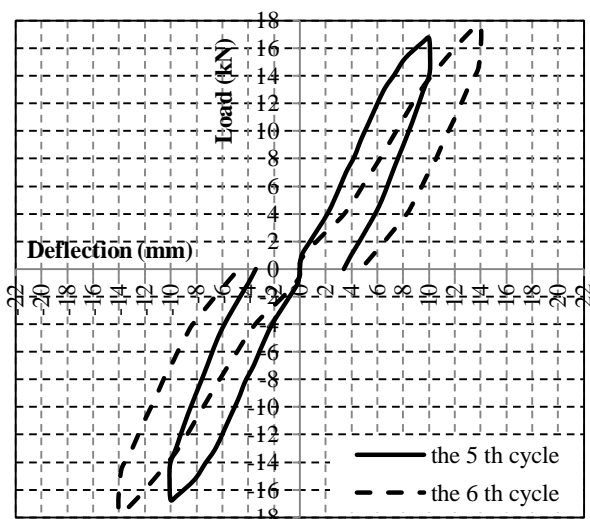


Figure 23. Load- deflection curve of the 5<sup>th</sup> and 6<sup>th</sup> cycles -  $\Delta_1$

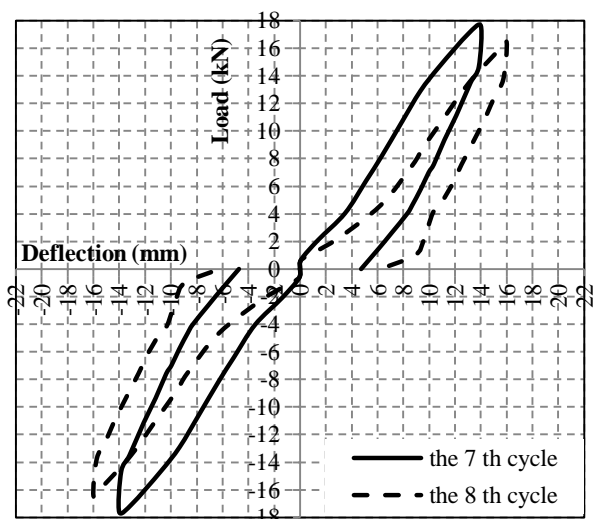


Figure 24. Load- deflection curve of the 7<sup>th</sup> and 8<sup>th</sup> cycles -  $\Delta_1$

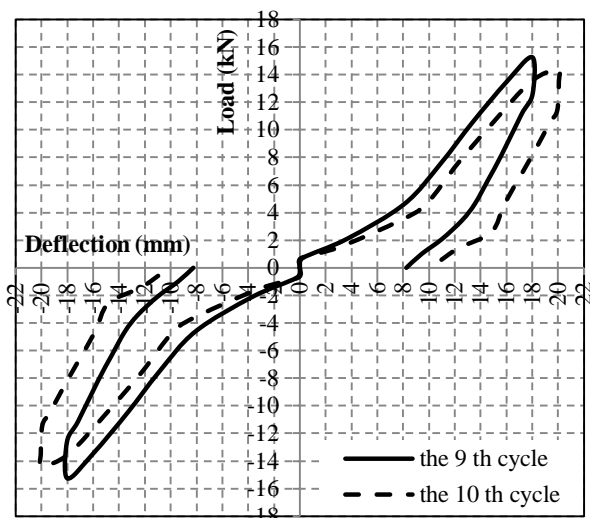


Figure 25. Load- deflection curve of the 9<sup>th</sup> and 10<sup>th</sup> cycles -  $\Delta_1$

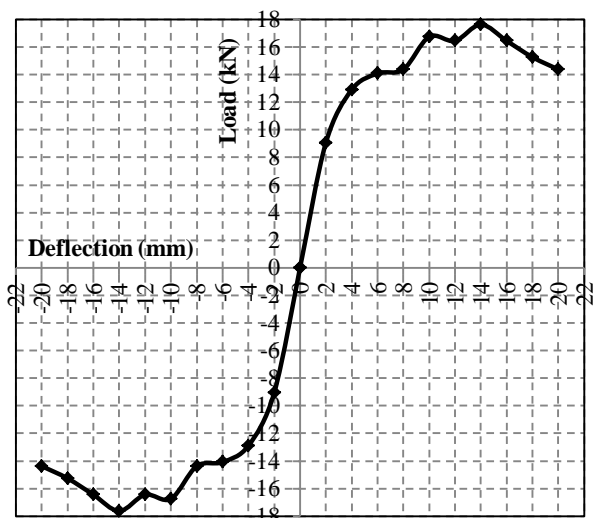


Figure 26. Peaks of load- deflection curves of the tested specimen -  $\Delta_1$

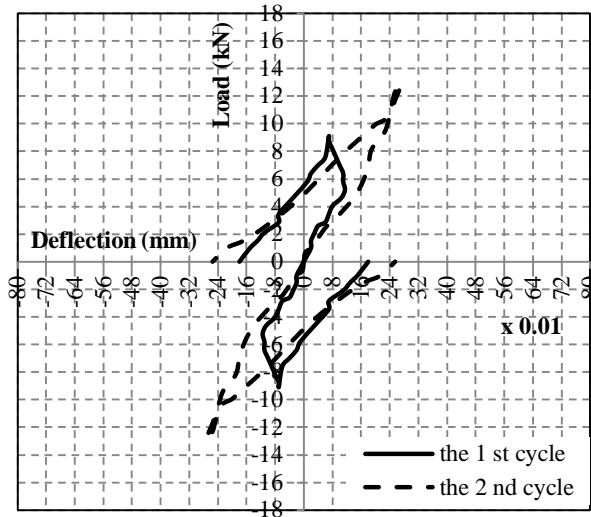


Figure 27. Load- deflection curve of the 1<sup>st</sup> and 2<sup>nd</sup> cycles-  $\Delta_2$

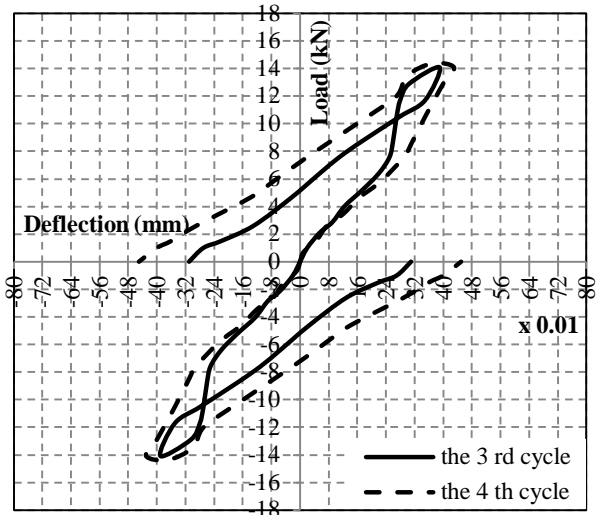


Figure 28. Load- deflection curve of the 3<sup>rd</sup> and 4<sup>th</sup> cycles-  $\Delta_2$

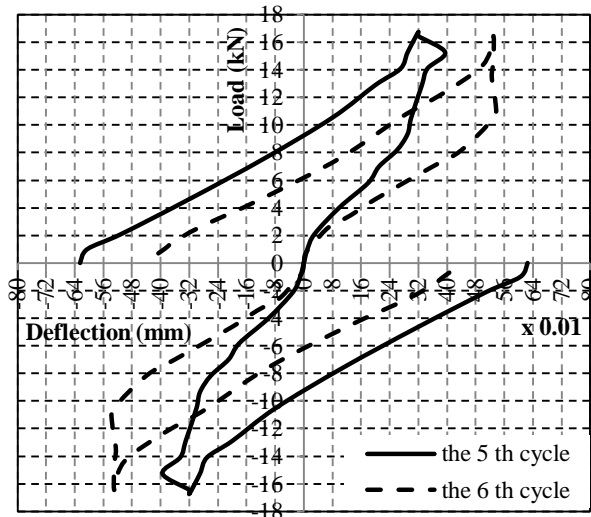


Figure 29. Load- deflection curve of the 5<sup>th</sup> and 6<sup>th</sup> cycles-  $\Delta_2$

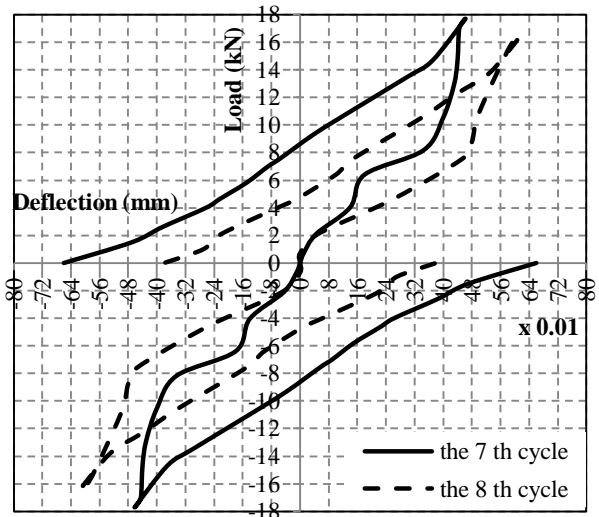


Figure 30. Load- deflection curve of the 7<sup>th</sup> and 8<sup>th</sup> cycles-  $\Delta_2$

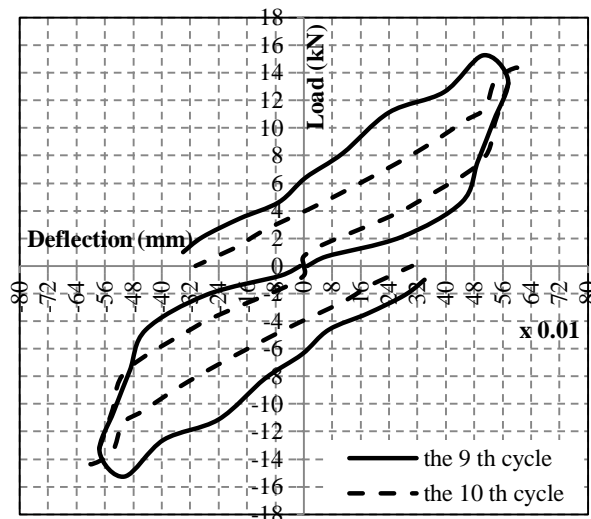


Figure 31. Load- deflection curve of the 9<sup>th</sup> and 10<sup>th</sup> cycles-  $\Delta_2$

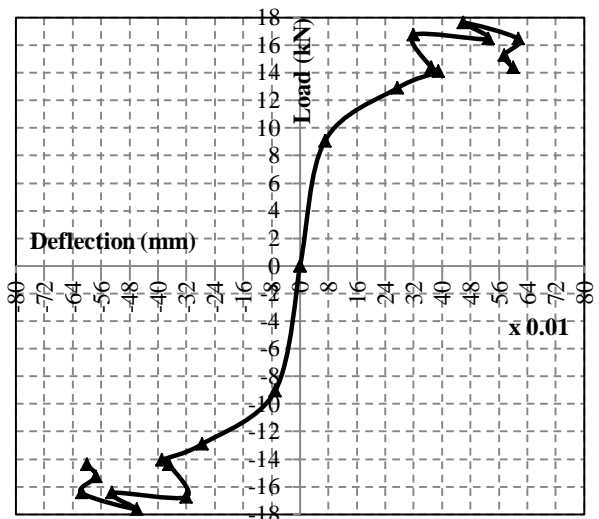


Figure 32. Peaks of load- deflection curves of the tested specimen-  $\Delta_2$

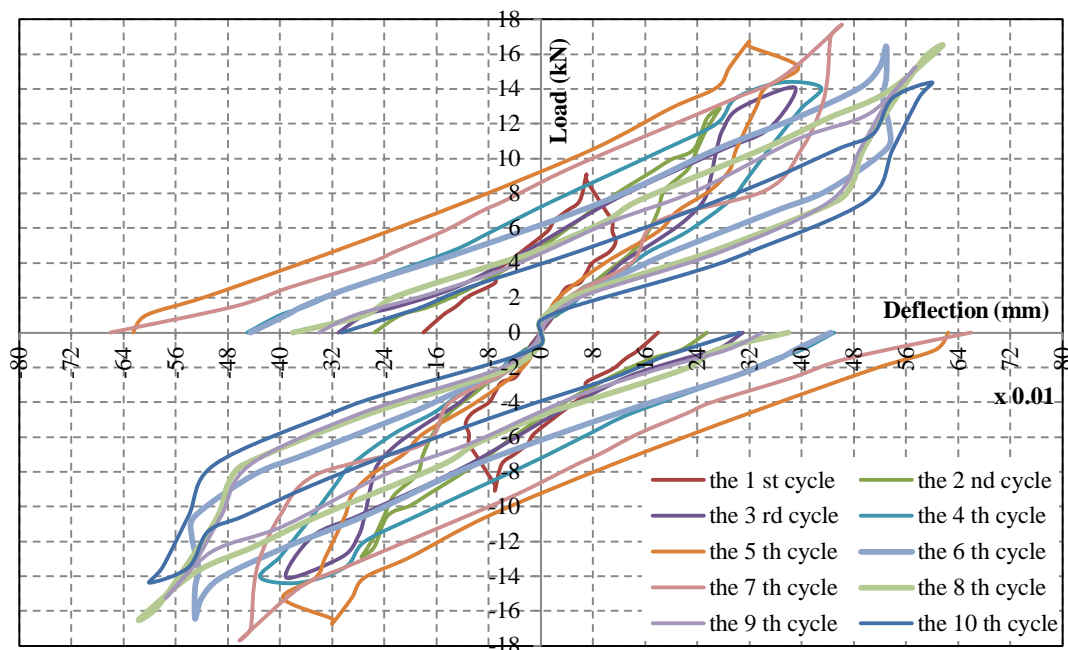


Figure 33. Load- deflection relationships of all cycles for the tested specimen- $\Delta_2$

#### 4. Conclusion

In this article, the effect of the eccentricity of the beam on behavior of the reinforced concrete beam column connection was investigated experimentally. The program consisted of one specimen. The crack pattern of the tested specimen was recorded in each cycle separately. The vertical deflection of the free end beam and horizontal displacement of column were drawn versus the cyclic load at each cycle separately. The main conclusion was discussed as summarized below:

- It was found that the cracks propagation was developed almost in the joint side closed to the beam eccentricity.
- The deflection rate of the beam and the column at any current cycle was higher than the previous cycle.
- When the free end of the beam moved 20 mm down ward, the middle of the upper column moved 0.5 mm to the right.
- The relationship between the load and deflection was nonlinear during the loading, while it was linear during the load releasing.

#### 5. References

- [1] ACI Committee 318. Recommendations for Design of Beam-Column Connections in Monolithic Reinforced Concrete Structures (ACI 352R-2). Detroit, MI: American Concrete Institute (2002).
- [2] Kiran, Ravi, and Giovacchino Genesio. "A case study on pre 1970s constructed concrete exterior beam-column joints." *Case Studies in Structural Engineering* 1 (2014): 20-25.
- [3] Masi, Angelo, Giuseppe Santarsiero, Gian Piero Lignola, and Gerardo M. Verderame. "Study of the seismic behavior of external RC beam-column joints through experimental tests and numerical simulations." *Engineering Structures* 52 (2013): 207-219.
- [4] Burak, B. U. R. C. U., and JAMES K. Wight. "Experimental investigation of eccentric reinforced concrete beam-column-slab connections under earthquake loading." In *Proceedings of the 13th World Conference on Earthquake Engineering*, Paper, no. 2150. 2004.
- [5] Dhakal, Rajesh Prasad, Tso-Chien Pan, Paulus Irawan, Keh-Chyuan Tsai, Ker-Chun Lin, and Chui-Hsin Chen. "Experimental study on the dynamic response of gravity-designed reinforced concrete connections." *Engineering Structures* 27, no. 1 (2005): 75-87.
- [6] Elsouri, A. M., and M. H. Harajli. "Seismic response of exterior RC wide beam-narrow column joints: earthquake-resistant versus as-built joints." *Engineering Structures* 57 (2013): 394-405.
- [7] Chalioris, Constantin E., Maria J. Favvata, and Chris G. Karayannis. "Reinforced concrete beam-column joints with crossed inclined bars under cyclic deformations." *Earthquake Engineering & Structural Dynamics* 37, no. 6 (2008): 881-897.
- [8] Fu, Jianping, Tao Chen, Zheng Wang, and Shaoliang Bai. "Effect of axial load ratio on seismic behavior of interior beam-

column joints." In Proc. 12th world conf. earthquake eng. 2000.

[9] Egyptian Code for Design and Construction of Reinforced Concrete Structures, (ECP 203-2007) 2012.

[10] Prakash Panjwani and S.K. DUBEY "Study of Reinforced Concrete Beam-Column Joint" International Journal of Engineering Research, Volume No.4, Issue No.6, pp : 321-324, 2015.

[11] Er. Khairnar Nilesh K, Kandekar S.B., and R.S.Talikoti " Experimental Investigation on Torsional Behaviour of Beam-Column Joint Wrapped with Aramid fibre" International Journal of Modern Trends in Engineering and Research (IJMTER) Volume 02, Issue 08, PP: 2393-8161, 2015.